Effects of Species of Non-meltable and Meltable Materials and Their Physical Properties on Granulatability in Tumbling Melt Granulation Method

Toru MAEJIMA,* Takashi OSAWA, Kingo NAKAJIMA, and Masao KOBAYASHI

Pharmaceutics Research Laboratory, Tanabe Seiyaku Co., Ltd., 3–16–89 Kashima, Yodogawa-ku, Osaka 532, Japan.
Received April 25, 1997; accepted July 24, 1997

Factors affecting granulatabilities in the tumbling melt granulation (TMG) method for the preparation of spherical beads without using any solvent were investigated. Beads of ten kinds of non-meltable materials were prepared using hydrogenated rape oil (HRO) as binder by changing the mixing ratio of the meltable material (X_M), and the recovery percent (Rec%) and yield percent (Ysc%) of the non-agglomerated core beads were evaluated. In all the powders, both Rec% and Ysc% were excellent with choice of the optimum mixing ratio (X_{op}), suggesting the great advantage of this method. The values of liquid saturation of the coated layer (ϕ) at X_{op} were calculated as around 0.4 in bisbentiamine, cornstarch, lactose, talc, titanium dioxide, and zinc oxide; and around 0.6 in the four cellulose derivatives. The high values in cellulose derivatives could be due to the penetration of the meltable materials into these powders. Thus, X_{op} seemed to be determined in ordinary powders by choosing X_M which would give the ϕ value of 0.4. The granulatability became worse as the viscosity of the meltable material increased, but the wettability evaluated by the liquid penetration method did not have much effect on the granulatability, in contrast with the wet granulation. From these results, the difference in the granulating mechanism between TMG and wet granulation was discussed.

Key words beads; tumbling melt granulation; centrifugal fluidizing granulator; packing characteristic; wettability; viscosity

We previously reported a new tumbling melt granulation (TMG) method for the preparation of spherical beads, in which the mixture of fine powder (non-meltable material) and wax (meltable material) was adhered to a seed material by a centrifugal-fluidizing granulator (CF).[1] This subsequent study was undertaken to determine the factors affecting the granulatability in more detail and to identify the granulating mechanism of this TMG method.

The cohesive or adhesive forces acting between the particles are very important in the granulation, and various forces are considered. When granules ranging in size from 100 to 1000 μm are prepared by wet granulation, the forces are known to be transmitted through a liquid bridge, viscous binder bridge, and a solid bridge.[2] The force transmitted through the liquid bridge is the most important of these since most pharmaceutical industries use the wet granulation method in manufacturing solid dosage forms.

In the funicular stage where the granulation is usually performed by this wet granulation method, the cohesive force transmitted through the liquid bridge is known to be proportional to the product of liquid saturation of voids (ϕ) and suction potential (P_s).[3] The decrease in P_s is ordinarily small in the funicular stage and thus ϕ is the most important index by which to determine the granulatability.[4–7]

Indeed, many studies indicated that the solid/liquid packing characteristics of a material is of primary importance in such wet granulation methods as tumbling, fluidized-bed, agitating, and extruding granulation.[8] A number of researchers have been tried to control the particle size of granules by monitoring the water content using an infrared moisture sensor, d.c. electrical conductance measurement, power consumption or torque measurement.[9–14] All of these methods are believed to detect the change of ϕ indirectly.

Concerning the melt granulation, Schaefer *et al.* reported that the liquid saturation of voids with molten material could be regarded as a granulating index similar to that of wet granulation.[15] Few systematic studies, however, have been performed on melt granulation. Thus we sought to identify the solid/liquid packing characteristics for the TMG method previously developed.

With regard to the factors caused by meltable materials, the spreading of meltable materials onto the surface of non-meltable material and the affinity of the meltable to the non-meltable material are important. The viscosity of binder solution greatly affected the property of the granules obtained in the wet granulation,[16,17] and seemed to affect the spreading of the binder on the surface. The addition of surfactant and additional agent was effective for the granulation of hydrophobic powder.[18–21] The crushing strength of the granules was also shown to be improved by the addition of alcohol to the binder solution.[3,22,23] These factors are believed to be related to the wettability of the binder solution to the powders. Thus, we investigated the effect of wettability and viscosity on the granulatability in the TMG method.

Experimental

Materials As seed materials, Nonpareil (20—24 mesh grade, 1.58 g/cm^3, Freund Industrial Co., Ltd., Tokyo, Japan) were used without any classification. The particle sizes of Nonpareil used in this study were as follows: over 840 μm, very few; 710 to 840 μm, 94—97%; under 710 μm, very few. As meltable materials, hydrogenated rape oil (HRO, Kawaken Fine Chemical, Tokyo, Japan), myristic acid (Katayama Chemical, Osaka, Japan), and polyethylene glycol 4000, 6000, and 20000 (PEG-4000, PEG-6000, and PEG-20000, Sanyo Kasei, Kyoto, Japan) were used. These meltable materials were of JP grade, except for myristic acid, which was of JPCI-II grade. All materials were passed through a 100-mesh sieve (149 μm) by Turbo Screener (type TS 125 × 200, Turbo Kogyo, Yokosuka, Japan).

As non-meltable materials, lactose (200M: DMV, The Netherlands), bisbentiamine (BB, JPC grade, Tanabe Seiyaku Co., Ltd., Osaka, Japan), talc (Nippon Talc Co., Ltd., Japan), cornstarch (Nippon Food Kakou,

* To whom correspondence should be addressed.

Japan), microcrystalline cellulose (MCC, avicel PH101, Asahikasei Kogyo, Japan), ethylcellulose (EC, N10-F, Shin-Etsu Chemical Co., Ltd., Tokyo, Japan), titanium dioxide (TiO_2, Titan Industry Co., Ltd., Japan), zinc oxide (ZnO, Sakai Chemical Industry Co., Ltd., Japan), hydroxypropylmethylcellulose acetate succinate (HPMC-AS(M), Shin-Etsu Chemical Co. Ltd., Tokyo, Japan), carboxymethylcellulose calcium (ECG-505, Nichirin Chemical Industry, Japan) and tipepidine hibenzate (TP, JP grade, Tanabe Seiyaku Co. Ltd., Osaka, Japan) were used. All non-meltable materials were used without further treatment.

The wettability of powder was evaluated by caprylic acid (Nippon Oil & Fats Co., Ltd., Tokyo, Japan), PEG-300, or rape oil (both from Katayama Chemical, Osaka, Japan) instead of higher fatty acid, PEG-6000, and HRO, respectively. They were liquid at room temperature.

Tumbling Melt Granulation (TMG) TMG was carried out using a centrifugal fluidizing granulator (CF-360S: rotor diameter 360 mm; Freund Industrial Co., Ltd., Tokyo, Japan). Three hundred grams of seed material (Nonpareil) was pre-heated in the CF by blowing hot slit air (rotating speed, 150 rpm; blower temperature, 90 °C; blower rate, 250 Nl/min). Ninety grams of a powdered mixture of meltable and non-meltable materials was gradually and successively fed to the driving bed of the seed material (feeding rate, 10 g/min). The meltable material was melted on the surface of the preheated seed material, and then this molten meltable material acting as a binder led the non-meltable material to adhere to the seed material. By continuous tumbling and heating, the resultant melt granulation layer was gradually compacted and the surface of the outer layer became smooth. The bed temperature was kept constant during the granulation process. After feeding the designated amount of the powder mixture, the resultant beads were removed from the CF and cooled at room temperature. They were then put through sieves with 350 and 1000 μm open diameter to remove the agglomerates and non-adhering fine powder.

Evaluation of Granulatability The granulatability was estimated for the following two values: the recovery % of granulation mass (Rec%) and the yield % of non-agglomerated core beads (Ysc%, fraction ranged from 350 μm to 1000 μm) against the charging amount of the seed material and the powdered mixture. When both Rec% and Ysc% were over 93%, the granulatability was regarded as excellent.

Evaluation of Powder Properties True density was determined by pycnometer (Autopycnometer 1320: Micromeritics/Shimadzu Co., Ltd., Kyoto, Japan). Apparent density was measured after packing the non-meltable material into a 50-ml graduated cylinder pressed tightly using a glass rod according to Iinoya.[24] Mean particle diameter of material was determined by Laser Granulometry (Granulometry model 715, Cilas Co., Ltd., France).

Evaluation of Beads Properties The shape of the resultant beads was observed by an optical microscope (Type SZH: Olympus, Tokyo, Japan). The crushing strength was determined by a particle hardness tester (GRANO: Okada Seiko Co., Ltd., Tokyo, Japan) at 100 μm/s of the measured speed using more than 100 beads, and was then calculated using the following equation of Hiramatsu *et al.*[25]:

$$\text{crushing strength} = 2.8 \cdot P/D \cdot \pi \quad (1)$$

where P is the hardness and D is the diameter of the bead.

Evaluation of Viscosity of Meltable Material The viscosities of the molten meltable materials were determined at 80 °C by a rotation viscometer (Digital Viscometer DVL-B, Tokyo Keiki Co., Ltd., Tokyo, Japan).

Evaluation of Wettability of Powder The wettability of drugs was determined by the liquid penetration method at 25 °C.[26-29] A glass tube packed with drug powder (inner diameter, 3.1 mm; length, 150 mm) was prepared and the bottom was dipped in caplyric acid, PEG-300, or rape oil. The length of flow in time t was measured at a fixed interval. This method is based on an equation derived by Washburn[30] (Eq. 2):

$$h^2 = (\gamma \cdot \cos\theta \cdot R \cdot t)/2\eta \quad (2)$$

where h is the length of flow in time t, η is the viscosity of the saturated solution, γ is the surface tension of the liquid, R is the mean radius of the capillary tube, and θ is the contact angle. Wettability was evaluated as immersional wetting ($\gamma \cdot \cos\theta$). $\gamma \cdot \cos\theta$ was calculated from the slope of the linear plot of h^2 *vs.* t. R was calculated by the following Eq. 3:

$$R = 2\varepsilon/((1-\varepsilon) \cdot Sw \cdot \rho) \quad (3)$$

where ε is the porosity of the powder bed (and was calculated from the weight and volume of the drugs filling the glass tube), Sw is the specific surface area, and ρ is the density of drug powder. Sw and ρ were determined by the air penetration method (Type SS-10, Shimadzu Co., Ltd.,) and Autopycnometer 1320 (Micromeritics/Shimadzu Co., Ltd.), respectively.

Results and Discussion

Effect of Solid/Liquid Packing Characteristics Determination of Optimum Mixing Ratio: We previously reported that the mixing ratio of meltable material in the mixture of non-meltable and meltable materials was a very important factor affecting the granulatability in the TMG method.[1] The mixing ratio has strong correlation with the solid/liquid packing characteristics of meltable and non-meltable materials. To clarify this effect on the granulatability, ten kinds of non-meltable materials with various powder properties (Table 1) were granulated with a variety of mixing ratios.

A mixture of hydrogenated rape oil (HRO) and non-meltable material adhered to nonpareil used as seed material as described in the Experimental section. The particle size of each powder and HRO were arranged so as to be less than one-sixth of seed material (nonpareil) as reported.[1]

The Rec% and Ysc% are plotted against the mixing ratio of HRO (X_M) in Fig. 1, where X_M is defined as the weight percent of meltable materials against the weight of the mixture of the meltable and non-meltable materials. As shown, the dependency of Rec% and Ysc% on X_M was classified into two types. One had the maximum point in both Rec% and Ysc% at the same X_M, and the optimum X_M (X_{op}) could be determined easily by these factors as shown for EC, cornstarch, lactose, ECG-505, MMC, and talc; the other did not show these clear maximum points, and X_{op} could not be determined by Rec% or Ysc% alone as shown for HPMC-AS, BB, TiO_2, and ZnO.

In the former six cases, part of the powder did not adhere to the seed materials and was removed from the CF together with the exhausting air when X_M was less than X_{op}. This was due to the lack of binder, and consequently Rec% and Ysc% had low value. On the contrary, when X_M was more than X_{op}, the seed materials agglomerated with each other and this caused a decrease of Ysc%. At that time, a part of the meltable and non-meltable materials attached to the wall or stator of the CF, resulting in the decrease of Rec%. Both these results were due to the excessive binder at high X_M value.

In the latter four cases, Ysc% decreased due to the serious agglomeration when X_M was more than a critical value, similar to that of the former cases. However, Rec% and Ysc% retained high value below the critical value of X_M, and consequently X_{op} could not be determined from Rec% and Ysc% alone. This seemed to be due to the fact that these powders had considerably high cohesive properties and could constitute the coating layer by the centrifugal force of the CF even when X_M was low. Thus, the crushing strength of beads obtained was measured and X_{op} was determined using the three parameters of the crushing strength, Rec%, and Ysc% in the latter four cases.

The effect of mixing ratio on the crushing strength is shown in Fig. 2 for these beads. In all of the four powders,

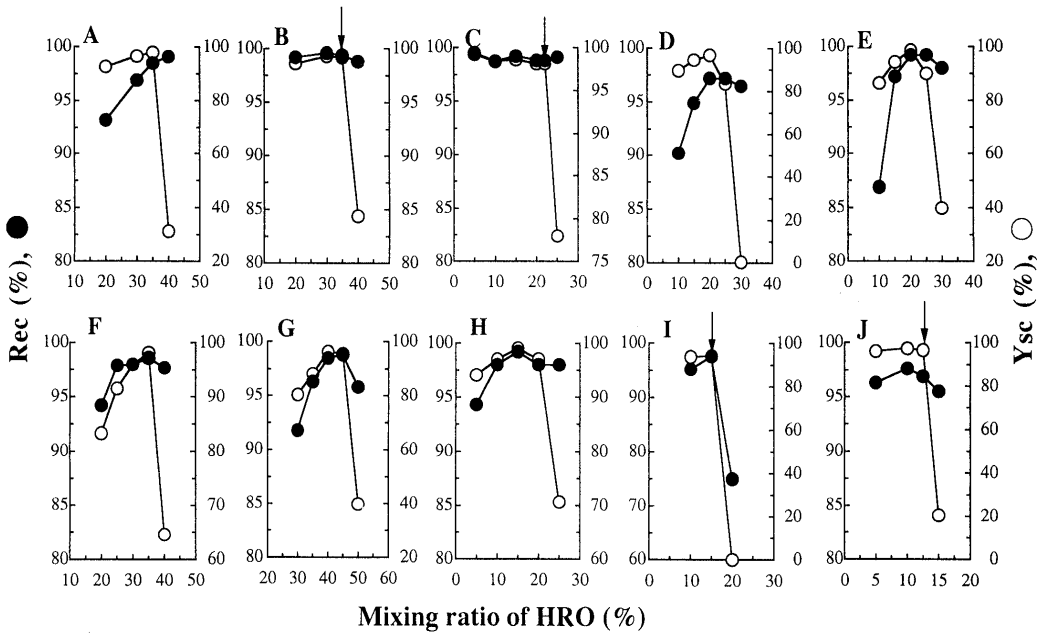

Fig. 1. Dependency of Rec% and Ysc% on Mixing Ratio of HRO

A, EC; B, HPMC-AS; C, BB; D, cornstarch; E, lactose; F, ECG-505; G, MMC; H, talc; I, TiO_2; J, ZnO. Arrows show the X_M at which the crushing strength was maximum.

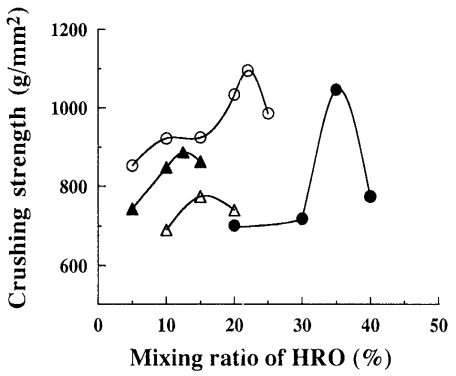

Fig. 2. Dependency of Crushing Strength on Mixing Ratio of HRO

●, HPMC-AS; ○, BB; △, TiO_2; ▲, ZnO.

Table 1. Powder Properties of Non-meltable Material Used for Preparation of Beads and Optimum Mixing Ratio of HRO

	D_{50} (μm)	D_{s1} (g/cm³)	D_{s2} (g/cm³)	X_{op} (%)
EC	4.5	1.26	0.486	35
HPMC-AS	5	1.34	0.525	35
BB	5.7	1.38	0.650	22
Cornstarch	13	1.41	0.728	20
Lactose	50	1.53	0.744	20
ECG-505	40	1.54	0.620	35
MMC	40	1.66	0.486	45
Talc	11	2.80	1.134	15
TiO_2	0.6	3.97	1.342	15
ZnO	1.1	5.74	1.750	12.5

D_{50}, mean particle size; D_{s1}, true density; D_{s2}, apparent density at the stage packed tightly with a rod; X_{op}, optimum mixing ratio.

the crushing strength increased with the increase of X_M, and then reached maximum at a certain value. In the range above this value, it decreased again. This seemed to be due to the coated layer being imperfectly densified by the centrifugal force of the CF when excess binder was used.

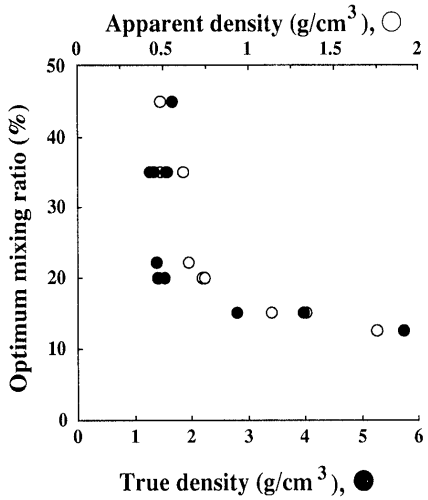

Fig. 3. Relationship between Optimum Mixing Ratio (X_{op}) and Density

●, true density; ○, apparent density.

Arrows in Fig. 1 mark the X_M where the crushing strength showed maximum . At these points both Rec% and Ysc% retained high values, and thus X_{op} in HPMC-AS, BB, TiO_2, and ZnO were determined to be 35%, 22%, 15%, and 12.5%, respectively.

The X_{op} are summarized in Table 1 together with the properties of the powders used. Using these data, the X_{op} were plotted against the true and the apparent density of non-meltable material (Fig. 3). The X_{op} tended to decrease with the increase of the true or apparent densities of the relevant non-meltable materials. Haramiishi *et al.*[31] reported that powder with larger density was granulated more easily in fluidized melt granulation, and consequently the amount of meltable material necessary for granulating was greatly affected by the density of powder. The results shown in Fig. 3 seem consistent with their results.

Consideration of Optimum Mixing Ratio: The relationship between the granulatability and the packing

characteristics of the solid/liquid system has been well studied in the wet granulation, but few studies have been carried out in the melt granulation. Thus, to determine the effect of solid/liquid packing characteristics on granulatability in the TMG, the term liquid saturation (ϕ) was calculated. Here, ϕ is defined as the ratio of the volume filled with the molten meltable material (V_m) against the void constituted among non-meltable material (V_0), V_m/V_0, as shown schematically in Fig. 4.

It was impossible to evaluate the packing characteristics directly for the case in which non-meltable materials were packed tightly by the forces generated in the CF. Therefore, we evaluated ϕ value assuming that the situation of non-meltable materials tumbled in the CF were the same as when they were packed tightly as described at the determination of apparent density in the Experimental section. As shown in Fig. 4, the apparent volume of coated layer without meltable material, V_{total}, is given by

$$V_{total} = V_s + V_0 \tag{4}$$

where V_s and V_0 are the volume occupied by non-meltable material and that of the void constituted among particles of non-meltable material, respectively. V_s and V_{total} are written as

$$V_s = W_s/D_{s1} \tag{5}$$

$$V_{total} = W_s/D_{s2} \tag{6}$$

where W_s is the weight of non-meltable material, and D_{s1} and D_{s2} are the true density and the apparent density of the non-meltable material, respectively. V_0 and the volume occupied by the molten meltable material, V_m, are written as

$$V_0 = (W_s/D_{s2}) - (W_s/D_{s1}) \tag{7}$$

$$V_m = W_m/D_{m1} \tag{8}$$

where W_m is the weight of meltable material and D_{m1} is the true density of meltable material in the molten stage. The total weight of the coated layers, W_{total}, W_s, and W_m is written as

$$W_{total} = W_s + W_m \tag{9}$$

$$W_s = (1 - X_M) \cdot W_{total} \tag{10}$$

$$W_m = X_M \cdot W_{total} \tag{11}$$

The liquid saturation, ϕ, is given by dividing Eq. 8 by Eq. 7 and combining with Eq. 10 and Eq. 11 as

$$\phi = \frac{V_m}{V_0} = \frac{W_m/D_{m1}}{(W_s/D_{s2}) - (W_s/D_{s1})} = \frac{X_M}{1 - X_M} \cdot \frac{D_{s1} \cdot D_{s2}}{D_{m1} \cdot (D_{s1} - D_{s2})} \tag{12}$$

Thus, ϕs were calculated by using Eq. 12 and the relationship betweenϕ and X_M is shown in Fig. 5. The experimental values of the optimum mixing ratios, X_{op}, are also shown by solid circles for each non-meltable material. In all the non-meltable materials with the exception of the cellulose derivatives, the liquid saturations at the optimum mixing ratio had almost the same value of 0.4 (Fig. 5A); in contrast, they were over 0.5 in the cellulose derivatives (Fig. 5B). This high value was presumed to be due to the fact that a part of molten

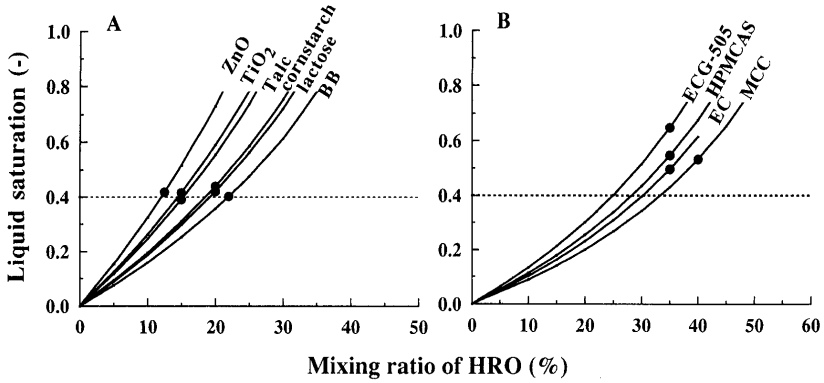

Fig. 4. Schematic Presentation of Packing Characteristics of Meltable and Non-meltable Material

The packing situation of non-meltable material without meltable material (A), and that where a part of the void was occupied with molten meltable material (B).

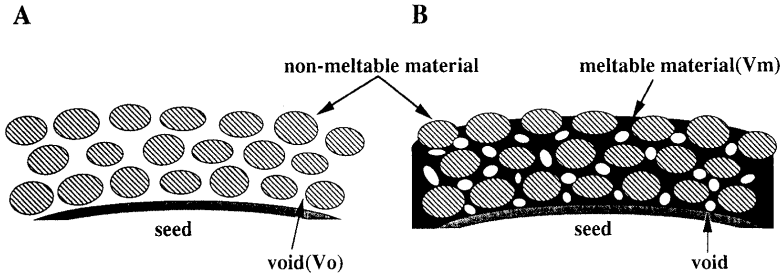

Fig. 5. Relationship between Mixing Ratio of Meltable Material and Liquid Saturation Calculated Using Eq. 12 in Various Non-meltable Materials

●, optimum mixing ratio obtained experimentally.

meltable material penetrated into the cellulose itself according to Haramiishi *et al.*[31]

From these results, it was concluded that X_{op} of the ordinary non-meltable materials having no special interaction with the meltable materials could be determined by choosing X_M which would give ϕ value of around 0.4.

Effect of Viscosity of Meltable Material The effect of viscosity on the granulatability was estimated using such meltable materials with different viscosities as myristic acid (mp, 58 °C), HRO (mp, 70 °C), PEG-4000 (mp, 55 °C), PEG-6000 (mp, 58 °C), and PEG-20000 (mp, 62 °C). Lactose was used as a non-meltable material and the mixing ratio X_M was fixed at 20%. The TMG was performed at 80 °C, where the temperature was at least 5 °C higher than each melting point. The Rec% and Ysc% are shown in Fig. 6 against the viscosity of meltable materials at 80 °C.

In the cases of myristic acid and HRO with low viscosity, the granulatabilities were excellent. As can be seen in PEGs of various viscosities, Rec% and Ysc% decreased with the increase of viscosity, indicating that more nonadherent powder and agglomeration of beads was generated by use of meltable material with higher viscosity.

The microphotographs of the beads obtained using these meltable materials are shown in Fig. 7. The beads became more concavoconvex and irregular with the increase of viscosity, which also suggested that the granulatability became better as viscosity decreased.

Schaefer and Mathiesen[32] also reported that the viscosity of meltable material greatly affected the granulatability in the melt pelletization in a high shear mixer. It was shown that a higher viscosity gave rise to a lower initial agglomerate growth due to the slower distribution of the molten binder and a higher agglomerate growth rate followed after the distribution had been completed. And the surface plasticity of pellets became lower at a higher viscosity, resulting in pellets of more irregular shape.

In this TMG, the viscosity affected the granulatability as well as the melt pelletization. The decrease of Rec% at higher viscosity showed the increase of nonadherent powder which was exhausted from the powder bed with the slit air, and this was ascribed to a poor binder distribution at the initial stage and a low surface plasticity of beads. The decrease of Ysc% in higher viscosity was believed due to the increase of the agglomeration of beads generated after completion of the distribution of the molten binder. Further, the shape of beads was more irregular at higher viscosity and this was also in agreement with Schaefer and Mathiesen.[32]

Effect of Wettability It is known that the adhesive force generated by granulating moisture greatly affects the formation of the granule. The crushing strength of beads (σ) is theoretically described as

$$\sigma = C\frac{\gamma}{d}\cdot\cos\theta\cdot\frac{1-\varepsilon}{\varepsilon}\cdot\phi\cdot F(\phi) \qquad (13)$$

where C is a constant, d is the radius of constituted particle, ε is porosity of powder bed, ϕ is liquid saturation of voids, and $F(\phi)$ is the function of ϕ.[33-34] The term of $\gamma\cdot\cos\theta$

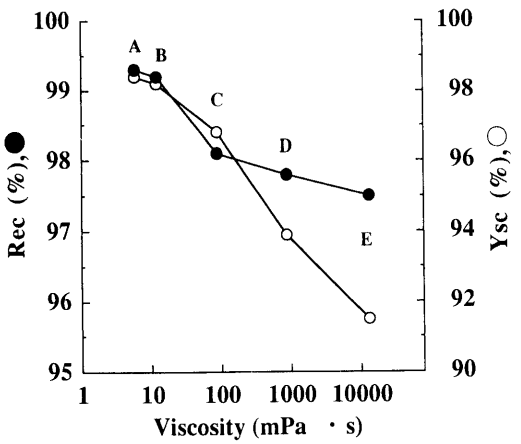

Fig. 6. Effect of Viscosity of Meltable Materials Determined in Molten State on Granulatability

●, Rec%; ○, Ysc%; A, myristic acid; B, HRO; C, PEG-4000; D, PEG-6000; E, PEG-20000.

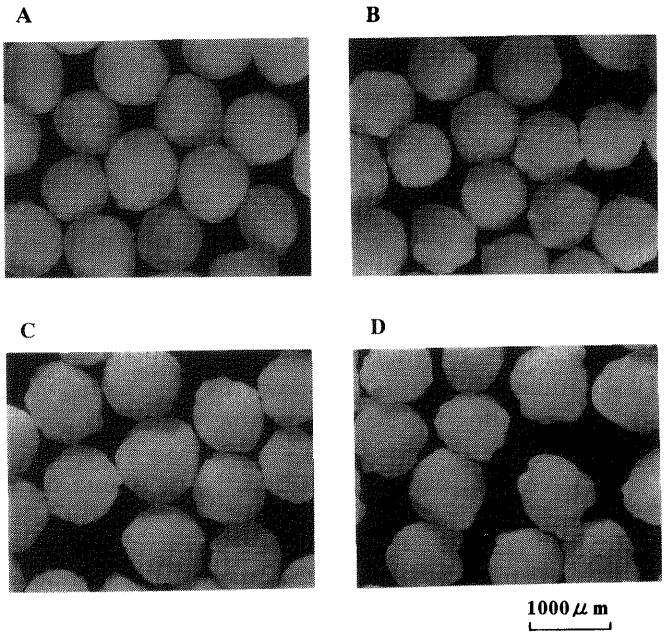

Fig. 7. Microphotographs of Beads Prepared Using Different Meltable Materials with Various Viscosities

A, HRO; B, PEG-4000; C, PEG-6000; D, PEG-20000.

in Eq. 13 is known as immersional wetting. It was presumed from Eq. 13 that immersional wetting had a strong effect on the granulatability; thus we tried to estimate the immersional wettings for non-meltable materials against the molten meltable materials. However, it was difficult to determine these directly at the high temperature used to perform TMG. Therefore, liquid materials of analogous chemical structure with solid meltable materials at room temperature were chosen and the immersional wetting against meltable materials was determined. PEG-300, caprylic acid, and rape oil were used as representatives of polyethylene glycols, higher fatty acids, and triglycerides, respectively, and the immersional wetting for non-meltable materials with different hydrophilicities (shown in Table 2) was determined.

According to Washburn Eq. 2, good linearity held in all cases (coefficient of correlation $\gg$0.998) with the

Table 2. Immersional Wetting of Non-meltable Materials against Liquid Molecules Having Analogous Chemical Structure with Meltable Materials Used in This Study

	Sw (cm^2/g)	ε	PEG-300		Caprylic acid		Rape oil	
			Slope ($\times 10^{-4}$)	IW (dyn/cm)	Slope ($\times 10^{-4}$)	IW (dyn/cm)	Slope ($\times 10^{-4}$)	IW (dyn/cm)
Lactose	4286	0.430	13.4	8.04	82.5	3.92	11	5.57
BB	12840	0.638	11.7	8.18	Solved		8.7	5.12
TP	9620	0.581	Solved		85.4	4.29	9.8	5.26
Talc	12322	0.745	1.9	1.55	25.1	1.62	2.6	1.63

Sw, specific surface area; ε, porosity of powder bed; slope, $\gamma \cdot \cos\theta \cdot R/2\eta$ (cm^2/s); IW, immersional wetting.

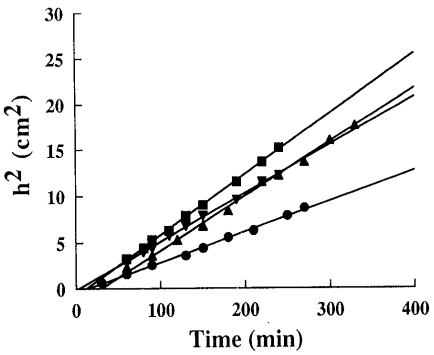

Fig. 8. Relationship between Flow Length in Powder Bed and Immersed Time

Non-meltable material: ●, talc; ▼, BB; ▲, TP; ■, lactose. As meltable material, rape oil was used.

exception of PEG-TP and caprylic acid-BB where a part of non-meltable materials was solved with these liquids. The plotting for rape oil is shown in Fig. 7, and immersional wetting calculated from the slope is summarized in Table 2.

In lactose, BB, and TP, the $\gamma \cdot \cos\theta$s were more than 4.0 dyn/cm in all the meltable materials in the order of PEG-300 > rape oil > caprylic acid. The values in talc were always the lowest among the four powders and were less than 1.6 dyn/cm in all the liquids.

We previously reported[35] that the granulatabilities of slightly water-soluble drugs in wet granulation were improved greatly by changing the solvent of binder from water to 30% ethanol solution where the $\gamma \cdot \cos\theta$ was maximum (the value was more than 2.5 dyn/cm). In this TMG, the values in lactose, BB, and TP were more than 2.5 dyn/cm in all cases, and thus good granulatability could be obtained. However, talc also gave excellent granulatability although it took a very small value (1.6 dyn/cm) for all liquids. This result is believed due to the following: 1) The adhesive force of binder should be stronger in TMG than that in wet granulation, since meltable material itself acts as a binder in the former, while binder is diluted with solvent in the latter. 2) In the wet granulation, drying immediately follows spraying of the binder solution, and the time for penetration of binder into the void and spreading on the powder surface would be much shorter. In TMG, however, the meltable material is not evaporated and can penetrate and spread during the entire granulating process; thus the adhesion and the deformation of coated material would proceed more effectively.

At any rate, the granulation in the TMG method proceeded well in the stage where the liquid saturation was almost 0.4, except with the cellulose derivatives. Thus, X_{op} could be estimated easily from the true and apparent densities for the ordinary non-meltable material having no specific interaction with the meltable material. Further, in the wet powder coating granulation, strict control of quantities of both the feeding powder and the spraying binder solution is very important, while only control of the feeding powder is critical in TMG if the optimum mixing ratio is fixed. This means that process control is much simpler in TMG than in wet granulation, and that TMG can be widely and easily applied to the granulation of many kinds of powders with various properties.

References

1) Maejima T., Osawa T., Nakajma K., Kobayashi M., *Chem. Pharm. Bull.*, **45**, 518—524 (1997).
2) Rumpf H., *Chem. Ing. Tech.*, **30**, 144—158 (1958).
3) Newitt D. M., Conway-Jones J. M., *Trans. Instn. Chem. Engrs.*, **36**, 422—442 (1958).
4) Toyoshima S, Watanabe S., Matsuo K., Kasai M., *Yakugaku Zasshi*, **91**, 1088—1091 (1971).
5) Harrison P. J., Newton J. M., Rowe R. C., *J. Pharm. Pharmacol.*, **37**, 81—83 (1985).
6) Watano S., Terashita K., Miyanami K., *Chem. Pharm. Bull.*, **42**, 1302—1307 (1992).
7) Aoki S., Okamoto A., Nemoto M., Yoshida T., Danjo K., Sunada H., Ostuka A., *Yakuzaigaku*, **53**, 194—199 (1993).
8) Tohata H. (ed.), "Zoryu Handbook," Omu Company, Tokyo, 1991, p. 15.
9) Watano S., Terashita K., Miyanami K., *Chem. Pharm. Bull.*, **39**, 1013—1017 (1991).
10) Funakoshi Y., Yamamoto M., Matsumura Y., Komeda H., *Powder Technol.*, **27**, 13—21 (1980).
11) Leuenberger H., Bier H.P., Sucker H., *Pharm. Technol.*, **2**, 35—42 (1979).
12) Terashita K., Yasumoto M., Miyanami K., *Yakugaku Zasshi*, **105**, 1166—1172 (1985).
13) Tapper G. I., Lindberg N. O., *Acta Pharm. Suec.*, **23**, 47—56 (1985).
14) Yoneyama T., Nakajima K., Abstract of Papers, The 106th Annual Meeting of Pharmaceutical Society of Japan, Chiba, April 1986, p. 564.
15) Schaefer T., Holm P., Kristensen H. G., *Drug Dev. Ind. Pharm.*, **16**, 1249—1277 (1990).
16) Tohata H. (ed.), "Zoryu Binran," Omu Company, Tokyo, 1975, p. 261.
17) Herman J., Remon J. P., *Drug Dev. Ind. Pharm.*, **14**, 1221—1234 (1988).
18) Tohata H. (ed.), "Saishin Zoryugijutsu no Jissai," Koubundo, Tokyo, 1984, p. 250.
19) Femi-Oyewo M. N., *Int. J. Pharmaceut.*, **40**, 73—79 (1987).
20) Tohata H. (ed.), "Zoryu Hand Book," Omu Company, Tokyo, 1991, p. 137.
21) Jaiyeoba K. T., Spring M. S., *J. Pharm. Pharmacol.*, **32**, 386—388

(1980).
22) Wells J. I., Walker C. V., *Int. J. Pharm.*, **15**, 97—111 (1983).
23) Wikberg M., Alderborn G. A., *Int. J. Pharm.*, **63**, 23—27 (1990).
24) Iinoya K. (ed.), "Funtaikogaku Handbook," Asakura, Tokyo, 1965, p. 103.
25) Hiramatsu Y., Oka Y., and Kiyama H., *Nippon Kogyo Kaishi*, **81**, 1024—1030 (1965).
26) Studebaker M. L., Snow C. W., *J. Phys. Chem.*, **59**, 973—976 (1955).
27) Buckton G., Newton J. M., *J. Pharm. Pharmacol.*, **37**, 605—609 (1985).
28) Buckton G., Newton J. M., *J. Pharm. Pharmacol.*, **38**, 329—334 (1986).
29) Nakagawa M., Furuuchi M., Miwa K., Gotoh K., *J. Soc. Tecnol. Jpn.*, **23**, 845—849 (1986).
30) Washburn E. W., *Phys. Rev.*, **17**, 273—283 (1921).
31) Haramiishi Y., Kitazawa Y., Kasai M., Kataoka K., *Yakugaku Zasshi*, **111**, 515—523 (1991).
32) Schaefer T., Mathiesen C., *Int. J. Pharmaceut.*, **139**, 125—138 (1996).
33) Tohata H. (ed.), "Saishin Zoryugijutsu no Jissai," Koubundo, Tokyo, 1984, p. 19.
34) Kubota N., Kawakami T., Ohtani S., *Kagaku Kogaku*, **32**, 822—824 (1968).
35) Maejima T., Osawa T., Kobayashi M., Noda K., *Chem. Pharm. Bull.*, **40**, 488—492 (1992).